SCIENCE CHINA
Information Sciences

• **Supplementary File** •

Distributed Adaptive Resilient Formation Control for Nonlinear Multi-Agent Systems under DoS Attacks

Hao Wen, Yongming Li & Shaocheng Tong*

College of Science, Liaoning University of Technology, Jinzhou 121001, China

Appendix A

Appendix A.1 Communication Network Topology

Suppose the communication topology $\mathcal{G} = (\mathcal{V}, \mathcal{E})$ is an undirected graph, where $\mathcal{V} = \{1, 2, \dots, N\}$ denots the set of agents, $\mathcal{E} = \{(i,j)|i \in \mathcal{V}, j \in \mathcal{V}\}$ is the set of edges between agents. $(i,j) \in \mathcal{E}$ represents that agent i and agent j can exchange information. Let the neighbor set of i be denoted as $\mathcal{N}_i = \{j \in \mathcal{V} : (i,j) \in \mathcal{E}\}$. The adjacency matrix is $\mathcal{A} = [a_{ij}] \in \mathbb{R}^{N\times N}$, where $a_{ij} > 0$ if $(i,j) \in \mathcal{E}, i \neq j$, and $a_{ij} = 0$, otherwise. The in-degree matrix is $\mathcal{D} = diag\{d_1, d_2, \dots, d_N\}$, where $d_i = \sum_{j=1}^{N} a_{ij}$. Define the Laplacian matrix as $\mathcal{L} = \mathcal{D} - \mathcal{A}$. If there exists a path composed of $\{(i,a), (a,b), \dots, (c,d), (d,j)\} \subseteq \mathcal{E}$ between any two agent i and j, the graph $\mathcal{G}$ is called connected. Define $\mathcal{B} = diag\{\mu_1, \mu_2, \dots, \mu_N\}$, where $\mu_i > 0$ if agent i can obtain information from the leader, and $\mu_i = 0$, otherwise. Also define $\mathcal{H} = \mathcal{L} + \mathcal{B}$. From [1,2], we define a graph $\bar{G}$, which consists of the leader node, edges between leader and followers, and graph $\mathcal{G}$.

The communication topology is a switched one under DoS attacks, we define $\bar{\mathcal{G}}_{\sigma(t)}$ as the topology $\bar{G}$ at moment t, where $\sigma(t) : [0, \infty) \to \{1, \dots, m\}$ denotes the switching signal.

Appendix A.2 DoS attacks

When the communication channel is under attack, the information transmission between agents may be interrupted. Denote $\mathcal{T}_k^{ij} = [g_k^{ij}, g_k^{ij} + \xi_k^{ij})$ as the kth attack interval when edge (i,j) is blocked, where g_k^{ij} and ξ_k^{ij} represents the starting instant and the length of the kth DoS attack on edge (i,j), respectively. From [3–5], we define $\Lambda^{ij}(t_a, t_b) := \bigcup_{k=1}^{d_{ij}} \mathcal{T}_k^{ij} \bigcap [t_a, t_b)$ as the set of time intervals during $[t_a, t_b)$, in which communication on edge (i,j) is blocked, where d_{ij} is the number of attacks of the edge (i,j). Define $\Xi^{ij}(t_a, t_b)$ as the set of time intervals during $[t_a, t_b)$ where communication on edge (i,j) is connected. Define $n^{ij}(t_a, t_b)$ as the number of times that the attacks happen in $[t_a, t_b)$.

Define $a_{ij}^{\sigma} = 0$ if the edge (i,j) is attacked at moment t, otherwise $a_{ij}^{\sigma} = a_{ij}$, and μ_i^{σ} can be defined in the same manner. Futhermore, define $\mathcal{A}_\sigma = [a_{ij}^\sigma], \mathcal{D}_\sigma = diag\{d_1^\sigma, \dots, d_N^\sigma\}, d_i^\sigma = \sum_{j=1}^{N} a_{ij}^\sigma, \mathcal{L}_\sigma = \mathcal{A}_\sigma - \mathcal{D}_\sigma, \mathcal{B}_\sigma = diag\{\mu_1^\sigma, \dots, \mu_N^\sigma\}, \mathcal{H}_\sigma = \mathcal{L}_\sigma + \mathcal{B}_\sigma$.

Appendix B Proof of Lemma 2

According to Assumption 3, the number of attacks on the edge (i,j) in $[t_k, t_{k+1})$ is finite; therefore, the number of switches of topology is finite. Assume that the switching moments are $t_k^1, \dots, t_k^{m_k-1}$, the topology is fixed in $[t_k^i, t_k^{i+1})$.

For edge (i,j) in interval $[t_k, t_{k+1})$, the duration without attacks satisfies

$$\begin{aligned} |\Xi^{i,j}(t_k, t_{k+1})| &= t_{k+1} - t_k - |\Lambda^{i,j}(t_k, t_{k+1})| \\ &> \frac{T_D^{ij} - 1}{T_D^{ij}}(t_{k+1} - t_k) - \zeta_D^{ij} \\ &\geqslant \frac{T_D^{ij} - 1}{T_D^{ij}} \cdot \frac{2T_D^{ij}\zeta_D^{ij}}{T_D^{ij} - 1} - \zeta_D^{ij} \\ &= \zeta_D^{ij} > 0 \end{aligned} \tag{B1}$$

From the above inequality, it can be known that each edge in graph $\bar{G}$ is connected at least one in $[t_k, t_{k+1})$. Which means that $\bar{G} = \cup_{i=0}^{m_k} \bar{G}_{\sigma(t^i)}, t_k^0 = t_k, t_k^m = t_{k+1}$, thus the graph $\bar{G}_{\sigma(t)}$ is jointly connected. This proof is completed.

Appendix C Proof of Theorem 1

Define $e_{i,n+q} = \eta_{i,n+q} - \xi_i - r, e_{n+q} = [e_{1,n+q}^{\mathrm{T}}, \dots, e_{N,n+q}^{\mathrm{T}}]^{\mathrm{T}}$.

$$V_0 = \frac{1}{2} e_{n+q}^{\mathrm{T}} e_{n+q} \tag{C1}$$

The derivative of V_0 is

$$\dot{V}_0 = -c e_{n+q}^{\mathrm{T}} (\mathcal{H}_\sigma \otimes I_m) e_{n+q} \tag{C2}$$

* Corresponding author (email: jztongsc@163.com)

Because $\mathcal{H}_\sigma$ is a real symmetric matrix, there exists an orthogonal matrix T_σ such that $\Lambda_\sigma = T_\sigma^{\mathrm{T}}\mathcal{H}_\sigma T_\sigma$, $\Lambda_\sigma = diag(\lambda_N^\sigma, \ldots, \lambda_1^\sigma)$. From [6, 7], define λ^σ as the smallest non-zero eigenvalue of $\mathcal{H}_\sigma$. Define $\bar{e}_{n+q} = (T_\sigma \otimes I_m)e_{n+q}$, $l(\sigma) = \{k|\lambda_k^\sigma \neq 0\}$. When λ^σ exists, we obtain the following expression as

$$\dot{V}_0 = -c\bar{e}_{n+q}^{\mathrm{T}}(\Lambda_\sigma \otimes I_m)\bar{e}_{n+q} \leqslant -c\lambda^\sigma \sum_{i\in l(\sigma)} \bar{e}_{i,n+q}^{\mathrm{T}}\bar{e}_{i,n+q} \leqslant 0 \tag{C3}$$

When $\lambda_i^\sigma = 0, i = 1, \ldots, N$, one has

$$\dot{V}_0 = -c\bar{e}_{n+q}^{\mathrm{T}}(\Lambda_\sigma \otimes I_m)\bar{e}_{n+q} = 0 \tag{C4}$$

From (C3)-(C4), the sequence $V_0(t_k)$ is monotonic and bounded. According to the Cauchy convergence criterion, for any given $\varepsilon > 0$, there exists a constant $T_\varepsilon > 0$ such that

$$V_0(t_k) - V_0(t_{k+1}) < \varepsilon, t_k \geqslant T_\varepsilon \tag{C5}$$

According to (C3)-(C5), when $t_k \geqslant T_\varepsilon$, one has

$$c\min_\sigma(\lambda^\sigma)\int_{t_k}^{t_{k+1}} \sum_{i\in l(\sigma)} \bar{e}_{i,n+q}^{\mathrm{T}}\bar{e}_{i,n+q}ds \leqslant \int_{t_k}^{t_{k+1}} -\dot{V}_0 ds = V_0(t_k) - V_0(t_{k+1}) < \varepsilon, t_k \geqslant T_\varepsilon \tag{C6}$$

From Lemma 1, difine $\tau_k = \min(t_k^{i+1} - t_k^i), i = 0, \ldots, m_k - 1, \tau = min(\tau_k)$. According to (C6), one has

$$c\min_\sigma(\lambda^\sigma)\int_{t_k^i}^{t_k^i+\tau} \sum_{i\in l(\sigma(t_k^i))} \bar{e}_{i,n+q}^{\mathrm{T}}\bar{e}_{i,n+q}ds \leqslant c\min_\sigma(\lambda^\sigma)\int_{t_k}^{t_{k+1}} \sum_{i\in l(\sigma)} \bar{e}_{i,n+q}^{\mathrm{T}}\bar{e}_{i,n+q}ds < \varepsilon, t_k \geqslant T_\varepsilon \tag{C7}$$

By (C7), it follows that

$$\lim_{t\to\infty}\int_t^{t+\tau} \sum_{i\in l(\sigma(t_k^i))} \bar{e}_{i,n+q}^{\mathrm{T}}\bar{e}_{i,n+q}ds = 0, i = 0, \ldots, m_k \tag{C8}$$

From Lemma 1, the graph $\bar{G}_{\sigma(t)}$ is jointly connected in $[t_k, t_{k+1})$. Using Lemma 2, (C3) and (C8), we have

$$0 = \lim_{t\to\infty}\int_t^{t+\tau} \sum_{i\in l(\sigma(t_k^0))} \bar{e}_{i,n+q}^{\mathrm{T}}\bar{e}_{i,n+q}ds + \cdots + \lim_{t\to\infty}\int_t^{t+\tau} \sum_{i\in l(\sigma(t_k^{m_k}))} \bar{e}_{i,n+q}^{\mathrm{T}}\bar{e}_{i,n+q}ds \geqslant \lim_{t\to\infty}\int_t^{t+\tau} \sum_{i=1}^N \bar{e}_{i,n+q}^{\mathrm{T}}\bar{e}_{i,n+q}ds \geqslant 0 \tag{C9}$$

Based on the properties of orthogonal transformations, we obtain

$$0 = \lim_{t\to\infty}\int_t^{t+\tau} \sum_{i=1}^N \bar{e}_{i,n+q}^{\mathrm{T}}\bar{e}_{i,n+q}ds = \lim_{t\to\infty}\int_t^{t+\tau} e_{n+q}^{\mathrm{T}}e_{n+q}ds = \lim_{t\to\infty}\int_t^{t+\tau} 2V_0(s)ds \geqslant \lim_{t\to\infty} V_0(t+\tau)\int_t^{t+\tau} 2ds \geqslant 0 \tag{C10}$$

Therefore $\lim_{t\to\infty} V_0 = 0$. Define $e_{i,j} = \eta_{i,j} - \eta_{i,j+1}, j = 1, \ldots, n+q-1$, according to estimator (4), yields

$$\begin{aligned}
\dot{e}_{i,1} &= -\delta_i e_{i,1} + (S + \delta_i \cdot I)e_{i,2} \\
\dot{e}_{i,2} &= -\delta_i e_{i,2} + (S + \delta_i \cdot I)e_{i,3} \\
&\vdots \\
\dot{e}_{i,n+q} &= -\delta_i e_{i,n+q} + c\mu_i^\sigma e_{i,n+q} + c\sum_{j\in\mathcal{N}_i} a_{ij}^\sigma(e_{i,n+q} - e_{j,n+q})
\end{aligned} \tag{C11}$$

Because $e_{i,n+q}$ converges to zero, $e_{i,j}$ converges to zero.

Appendix D Proof of Theorem 2

Define the coordinate transformation as follows:

$$\begin{aligned}
z_{i,1} &= x_{i,1} - \hat{y}_i \\
z_{i,q} &= x_{i,q} - \alpha_{i,q-1} - \hat{y}_i^{(q-1)}
\end{aligned} \tag{D1}$$

where $q = 2, \ldots, n, i = 1, \ldots, N$ and $\alpha_{i,q-1}$ is the virtual control signal to be designed later.

Step 1: Construct the Lyapunov function candidate

$$V_1 = \sum_{i=1}^N \frac{1}{2}z_{i,1}^2 + \frac{1}{2}\widetilde{\theta}_i^{\mathrm{T}}\Gamma_i^{-1}\widetilde{\theta}_i \tag{D2}$$

where Γ_i is a positive-definite matrix, $\widetilde{\theta}_i = \theta_i - \hat{\theta}_i$, $\hat{\theta}_i$ is the estimation of θ_i. Its time derivative is

$$\dot{V}_1 = \sum_{i=1}^N z_{i,1}(z_{i,2} + \alpha_{i,1} + \varphi_{i,1}^{\mathrm{T}}\theta_i) - \widetilde{\theta}_i^{\mathrm{T}}\Gamma_i^{-1}\dot{\hat{\theta}}_i \tag{D3}$$

Design the virtual control signal $\alpha_{i,1}$ as

$$\alpha_{i,1} = -c_{i,1}z_{i,1} - \varphi_{i,1}^{\mathrm{T}}\hat{\theta}_i \tag{D4}$$

where $c_{i,1} > 0$ is a design parameter.

Subsituting (D4) into (D3), yields

$$\dot{V}_1 = \sum_{i=1}^{N} z_{i,1}z_{i,2} - c_{i,1}z_{i,1}^2 - \widetilde{\theta}_i^{\mathrm{T}}\Gamma_i^{-1}(\dot{\hat{\theta}}_i - \Gamma_i\tau_{i,1})$$

where $\tau_{i,1}$ is a turning function defined as

$$\tau_{i,1} = z_{i,1}\varphi_{i,1}^{\mathrm{T}} \tag{D5}$$

Step $q(q = 2, \dots, n-1)$: Choose the Lyapunov function candidate

$$V_q = V_{q-1} + \sum_{i=1}^{N}\frac{1}{2}z_{i,q}^2 \tag{D6}$$

The time derivative of V_q is

$$\dot{V}_q = \dot{V}_{q-1} + \sum_{i=1}^{N} z_{i,q}(z_{i,q+1} + \alpha_{i,q} + \varphi_{i,q}^{\mathrm{T}}\theta_i) - \sum_{i=1}^{N} z_{i,q}[\sum_{j=1}^{q-1}\frac{\partial\alpha_{i,q-1}}{\partial\hat{y}_i^{(j-1)}}\hat{y}_i^{(j)} + \frac{\partial\alpha_{i,q-1}}{\partial\hat{\theta}_i}\dot{\hat{\theta}}_i + \sum_{j=1}^{q-1}\frac{\partial\alpha_{i,q-1}}{\partial x_{i,j}}(x_{i,j+1} + \varphi_{i,j}^{\mathrm{T}}\hat{\theta}_i + \varphi_{i,j}^{\mathrm{T}}\widetilde{\theta}_i)] \tag{D7}$$

Design the virtual control signal $\alpha_{i,q}$ and the turning function $\tau_{i,q}$ as

$$\begin{aligned}\alpha_{i,q} = {} & -c_{i,q}z_{i,q} - \varphi_{i,q}^{\mathrm{T}}\hat{\theta}_i - z_{i,q-1} + \sum_{j=1}^{q-1}\frac{\partial\alpha_{i,q-1}}{\partial\hat{y}_i^{(j-1)}}\hat{y}_i^{(j)} \\ & + \sum_{j=1}^{q-1}\frac{\partial\alpha_{i,q-1}}{\partial x_{i,j}}(x_{i,j+1} + \varphi_{i,j}^{\mathrm{T}}\hat{\theta}_i) + \frac{\partial\alpha_{i,q-1}}{\partial\hat{\theta}_i}\Gamma_i\tau_{i,q} \\ & + \sum_{j=2}^{q-1} z_{i,j}\frac{\partial\alpha_{i,j-1}}{\partial\hat{\theta}_i}\Gamma_i(\varphi_{i,q}^{\mathrm{T}} - \sum_{j=1}^{q-1}\frac{\partial\alpha_{i,q-1}}{\partial x_{i,j}}\varphi_{i,j}^{\mathrm{T}})\end{aligned} \tag{D8}$$

$$\tau_{i,q} = \tau_{i,q-1} + z_{i,q}\varphi_{i,q}^{\mathrm{T}} - z_{i,q}\sum\nolimits_{j=1}^{q-1}\frac{\partial\alpha_{i,q-1}}{\partial x_{i,j}}\varphi_{i,j}^{\mathrm{T}} \tag{D9}$$

Subsituting (D8) into (D7), yields

$$\dot{V}_q = \sum_{i=1}^{N} z_{i,q}z_{i,q+1} + \sum_{j=1}^{q} -c_{i,j}z_{i,j}^2 - \widetilde{\theta}_i^{\mathrm{T}}\Gamma_i^{-1}(\dot{\hat{\theta}}_i - \Gamma_i\tau_{i,q}) + \sum_{j=2}^{q-1} z_{i,j}\frac{\partial\alpha_{i,j-1}}{\partial\hat{\theta}_i}(\Gamma_i\tau_{i,q} - \dot{\hat{\theta}}_i)$$

Step n: Consider the Lyapunov function candidate

$$V_n = V_{n-1} + \sum_{i=1}^{N}\frac{1}{2}z_{i,n}^2 \tag{D10}$$

Its time derivative can be described as

$$\dot{V}_n = \dot{V}_{n-1} + \sum_{i=1}^{N} z_{i,n}(u_i + \varphi_{i,n}^{\mathrm{T}}\theta_i - \hat{y}_i^{(n)}) - \sum_{i=1}^{N} z_{i,n}[\sum_{j=1}^{n-1}\frac{\partial\alpha_{i,n-1}}{\partial\hat{y}_i^{(j-1)}}\hat{y}_i^{(j)} + \frac{\partial\alpha_{i,n-1}}{\partial\hat{\theta}_i}\dot{\hat{\theta}}_i + \sum_{j=1}^{n-1}\frac{\partial\alpha_{i,n-1}}{\partial x_{i,j}}(x_{i,j+1} + \varphi_{i,j}^{\mathrm{T}}\hat{\theta}_i + \varphi_{i,j}^{\mathrm{T}}\widetilde{\theta}_i)] \tag{D11}$$

Design the controller u_i, parameter adaptive law $\dot{\hat{\theta}}_i$, and turning function $\tau_{i,n}$ as

$$\begin{aligned}u_i = {} & -c_{i,n}z_{i,n} - \varphi_{i,n}^{\mathrm{T}}\hat{\theta}_i - z_{i,n-1} + \hat{y}_i^{(n)} + \frac{\partial\alpha_{i,n-1}}{\partial\hat{\theta}_i}\Gamma_i\tau_{i,n} \\ & + \sum_{j=2}^{n-1} z_{i,j}\frac{\partial\alpha_{i,j-1}}{\partial\hat{\theta}_i}\Gamma_i(\varphi_{i,n}^{\mathrm{T}} - \sum_{j=1}^{n-1}\frac{\partial\alpha_{i,n-1}}{\partial x_{i,j}}\varphi_{i,j}^{\mathrm{T}}) \\ & + \sum_{j=1}^{n-1}\frac{\partial\alpha_{i,n-1}}{\partial\hat{y}_i^{(j-1)}}\hat{y}_i^{(j)} + \sum_{j=1}^{n-1}\frac{\partial\alpha_{i,n-1}}{\partial x_{i,j}}(x_{i,j+1} + \varphi_{i,j}^{\mathrm{T}}\hat{\theta}_i)\end{aligned} \tag{D12}$$

$$\dot{\hat{\theta}}_i = \tau_{i,n} \tag{D13}$$

$$\tau_{i,n} = \tau_{i,n-1} + z_{i,n}\varphi_{i,n}^{\mathrm{T}} - z_{i,n}\sum\nolimits_{j=1}^{n-1}\frac{\partial\alpha_{i,n-1}}{\partial x_{i,j}}\varphi_{i,j}^{\mathrm{T}} \tag{D14}$$

Subsituting (D12) and (D13) into (D11), we have

$$\dot{V}_n = \sum_{i=1}^{N}\sum_{j=1}^{n} -c_{i,j}z_{i,j}^2 \leqslant 0 \tag{D15}$$

From (D10) and (D15), it follows that $z_{i,j}, \widetilde{\theta}_i$ are bounded. From the definition of $\widetilde{\theta}_i$, $\hat{\theta}_i$ are bounded. By using Assumption 1, Theorem 1, and estimator (4), one has that $y, \hat{y}_i^{(q)}, q = 0, \dots, n$ are bounded. From (D4), $\alpha_{i,1}$ are bounded. By the definition of $z_{i,2}$, $x_{i,2}$ are bounded. Using the similar procedure, we can obtain that all signals are bounded. Based on the LaSalle-Yoshizawa Theorem, $z_{i,j}$ converge to zero asymptotically.

Appendix E Simulation study

Simulation Example: Consider the MASs composed of four followers and one leader, and the communication topology is exhibited in Figure E1.

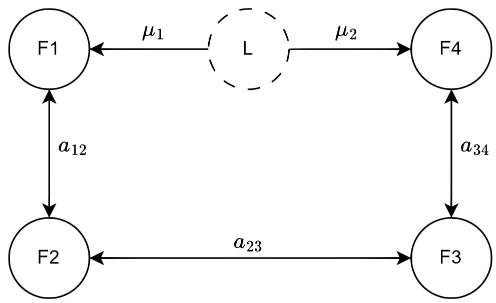

Figure E1 Communication topology

From Figure E1, we obtain the adjacency matrix $\mathcal{A}$ and the in-degree matrix $\mathcal{D}$ as follows:

$$\mathcal{A} = \begin{bmatrix} 0 & 1 & 0 & 0 \\ 1 & 0 & 1 & 0 \\ 0 & 1 & 0 & 1 \\ 0 & 0 & 1 & 0 \end{bmatrix}, \quad \mathcal{D} = \begin{bmatrix} 1 & 0 & 0 & 0 \\ 0 & 2 & 0 & 0 \\ 0 & 0 & 2 & 0 \\ 0 & 0 & 0 & 1 \end{bmatrix} \tag{E1}$$

The dynamics of the ith agent as follows:

$$\begin{cases} \dot{x}_{i,1} = x_{i,2} + \varphi_{i,1}^{\mathrm{T}}(x_{i,1})\theta_i, i = 1, \ldots, 4 \\ \dot{x}_{i,2} = u_i + \varphi_{i,2}^{\mathrm{T}}(\overline{x}_{i,2})\theta_i \\ y_i = x_{i,1} \end{cases} \tag{E2}$$

where $\varphi_{i,1}(x_{i,1}) = sin(x_{i,1})$, $\varphi_{i,2}(\overline{x}_{i,2}) = x_{i1} + x_{i2}$. $\theta_i = 2$.

The dynamics of virtual leadership are described as

$$\begin{aligned} \dot{r} &= \begin{bmatrix} 0 & 0.3 & 0.3 \\ -0.3 & 0 & 0 \\ -0.3 & 0 & 0 \end{bmatrix} r \\ y &= [0.2, -0.2, -0.2] r \end{aligned} \tag{E3}$$

The desired time-varying distances of the four agents with respect to the leader are $\xi_1 = [2+3cos(t), 2+3cos(t), 2+3cos(t)]^{\mathrm{T}}$, $\xi_2 = [2, 2, 2]^{\mathrm{T}}$, $\xi_3 = [3, 3, 3]^{\mathrm{T}}$, $\xi_4 = [4, 4, 4]^{\mathrm{T}}$.

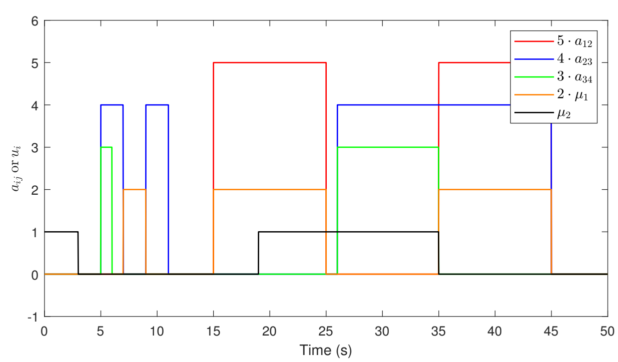

Figure E2 Active status of DoS attacks.

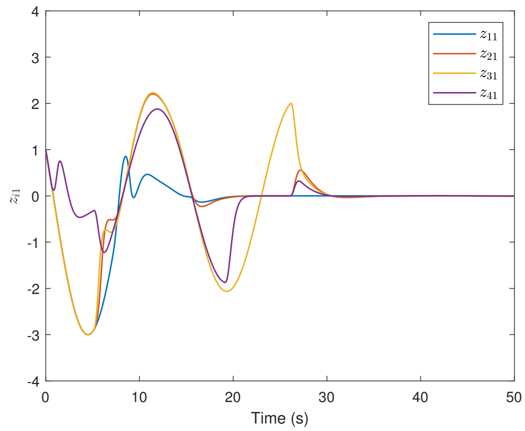

Figure E3 Tracking errors.

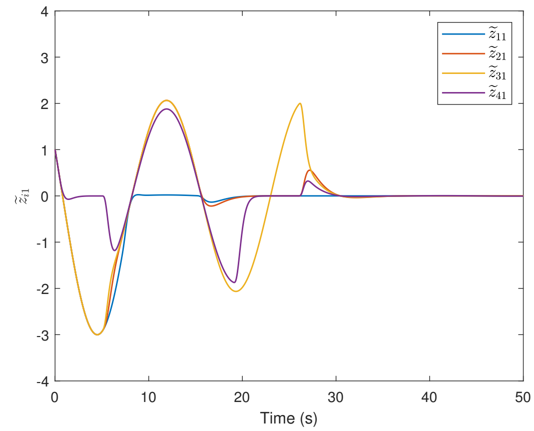

Figure E4 Estimator errors.

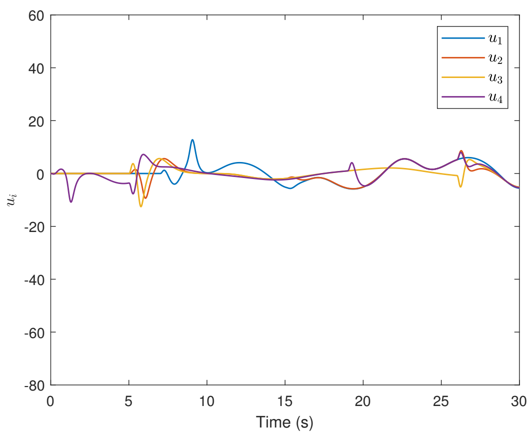

Figure E5 Trajectories of controller.

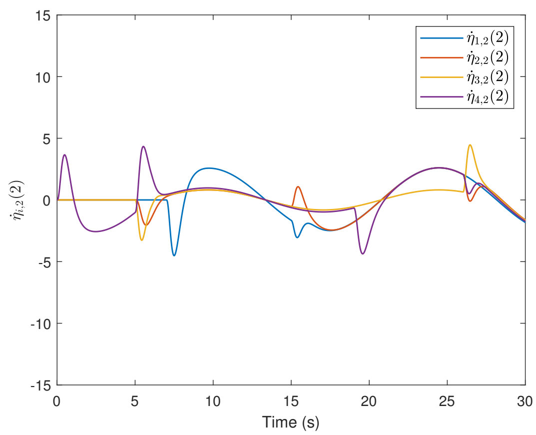

Figure E6 Trajectories of $\dot{\eta}_{i,2}(2)$.

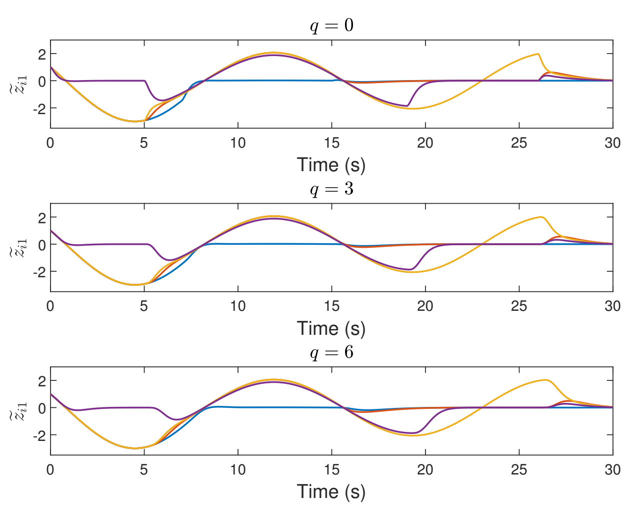

Figure E7 Estimator errors with different q.

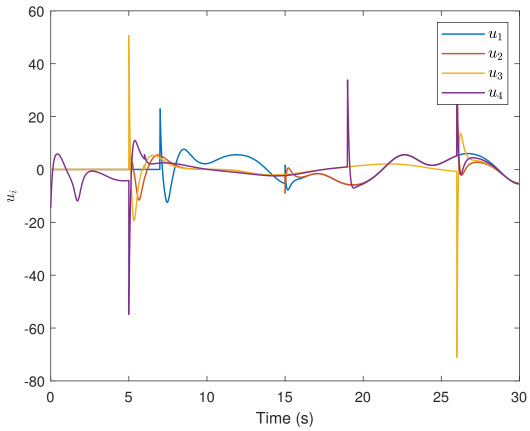

Figure E8 Trajectories of controller in [8].

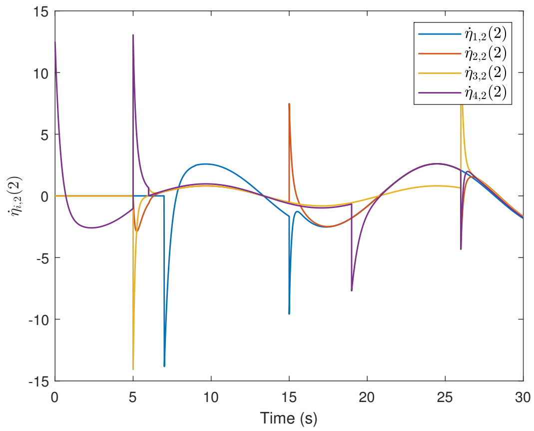

Figure E9 Trajectories of $\dot{\eta}_{i,2}(2)$ in [8].

Choose parameters $q = 3, c_{i,j} = 1, \delta_i = 7, c = 2.5, \Gamma_i = I$, and select initial conditions as $r(0) = [5, 5, 5]^{\mathrm{T}}$, the rest as zero vector or zero.

Figures.E2-E7 represent the simulation result. Figure E2 shows the active status of DoS attacks on different channels, where the channels represented by a_{ij} and μ_i are labeled in Figure E1. Figure E3 represents the curves of tracking errors, which indicates that the tracking errors converge. Figure E4 exhibits the curves of estimate errors, which indicates that the designed distributed resilient formation estimator can estimate the reference signal under DoS attacks. Figure.E5 presents the curves of controllers, which indicates that the curves of the controllers based on the estimator (4) are continuous under DoS attacks. Figure.E6 shows the curves of the second element of the n-th derivative of the estimator (4). Figure.E7 represents the estimator errors under different values of the parameter q in the estimator (4), which indicates that the convergence performance of the estimator (4) is insensitive to the choice of the parameter q.

To further show the merits of the proposed resilient control method, we apply the resilient control scheme in [8] to the above example. Then, we select $\xi_i = 0, i = 1, 2, 3, 4$. The remaining parameters, initial conditions, and active status of DoS attacks are the same as those in the previous simulation. The simulation results are exhibited in Figures. E8-E9. From Figures.E5-E6 and Figures.E8-E9, the proposed resilient controller is more smooth than [8].

References

1 Tao Liu, and Jie Huang. Leader-following attitude consensus of multiple rigid body systems subject to jointly connected switching networks. Automatica, 2018, 92: 63-71.
2 Wenying Xu, et al. Event-triggered schemes on leader-following consensus of general linear multiagent systems under different topologies. IEEE Transactions on Cybernetics, 2017, 47.1: 212-223.
3 Yongming Li, and Shaocheng Tong. Bumpless transfer distributed adaptive backstepping control of nonlinear multi-agent systems with circular filtering under DoS attacks. Automatica, 2023, 157: 111250.
4 Anyang Lu, and Guanghong Yang. Input-to-State Stabilizing Control for Cyber-Physical Systems With Multiple Transmission Channels Under Denial of Service. IEEE Transactions on Automatic Control, 2018, 63.6: 1813-1820.
5 Wenying Xu, et al. Event/self-triggered control for leader-following consensus over unreliable network with DoS attacks. IEEE Transactions on Neural Networks and Learning Systems, 2019, 30.10: 3137-3149.
6 Wei Ni, and Daizhan Cheng. Leader-following consensus of multi-agent systems under fixed and switching topologies. Systems & Control Letters, 2010, 59(3-4): 209-217.
7 Hui Yu, and Xiaohua Xia. Adaptive consensus of multi-agents in networks with jointly connected topologies. Automatica, 2012, 48.8: 1783-1790.
8 Dan Zhang, Chao Deng, and Gang Feng. Resilient cooperative output regulation for nonlinear multiagent systems under DoS attacks. IEEE Transactions on Automatic Control, 2022, 68.4: 2521-2528.